COMPDYN 2025
10th ECCOMAS Thematic Conference on
Computational Methods in Structural Dynamics and Earthquake Engineering
M. Papadrakakis, M. Fragiadakis (eds.)
Rhodes Island, Greece, 15-–18 June 2025

PREDICTION OF DAMPING RATIOS OF EXISTING RAILWAY BRIDGES USING REGRESSION METHODS AND MACHINE LEARNING

Ronny Behnke[1], **Günther Grunert**[1], **and Xiaohan Liu**[1]

[1]DB InfraGO AG
Caroline-Michaelis-Str. 5-11, 10115 Berlin, Germany
e-mail: ronny.behnke@deutschebahn.com

Keywords: Train-Bridge Interaction, Railway Bridges, Damping Ratio, Prediction, Regression, Machine Learning.

Abstract. *The realistic structural-dynamic description of railway bridges during train passage is crucial for the realistic evaluation of dynamic train-bridge compatibility. New vehicles (trains), especially in the high-speed range, can excite the existing railway bridges to undesirable resonance effects due to the regular sequence of axles when passing railway bridge constructions (periodic action). Therefore, the train-specific excitation behavior on existing railway bridges must be evaluated in the context of train-bridge compatibility as part of the technical network access process. In addition to cross-section values (distributed mass per meter of the bridge superstructure, bending stiffness of the cross-section), damping properties in the resonance case are particularly decisive. The approach of standard damping per material type according to DIN EN 1991-2:2010 usually results in damping values that are too low for existing bridges. From a series of measurement campaigns on reinforced concrete, pre-stressed concrete, and steel/steel composite bridges throughout Germany, it could be shown based on the evaluation of the vibration behavior of the railway bridges after train passage (free decay phase) that the identified (measured) damping values (damping ratio D) are usually higher than the standard damping according to DIN EN 1991-2:2010 (to be applied for the design of new construction projects). This contribution proposes a methodology for applying more realistic prediction values for railway bridges based on previous measurement results as part of the dynamic bridge compatibility check of new vehicles in the context of the technical network access. First, an overview of available measured values for railway bridges in the DB InfraGO AG railway network (Germany) is provided. The proposed damping values for existing railway bridges that have not yet been measured are predicted using multidimensional regression methods, considering the influencing variables of material type, year of construction, span length, static system and track type (e.g. ballast, slab track, direct rail fastening). Using a neural network approach, the outcome of machine learning (ML) is also compared with the regression results from multidimensional interpolation. A safety factor approach is finally discussed for practical application in a safety-relevant context.*

1 INTRODUCTION

As part of the technical network access in the area of the railway network of DB InfraGO AG (railway infrastructure manager in Germany), new trains must be examined for dynamic compatibility with the existing bridge infrastructure. At higher vehicle operating speeds, the dynamic component in the structural response from the train-bridge interaction increases, see e.g. [1]. The regular sequence of similar or even identical wheelset loads leads to periodic excitation of the bridge superstructure when trains pass (Fig. 1) and can exceed the available capacity of the load-bearing capacity (ultimate limit state – ULS) in the resonance case (excitation frequency corresponds to one of the bridge eigenfrequencies), see permissible limit speeds of quasi-static compatibility given in DIN EN 15528:2022, Table C.1. Furthermore, the current compatibility tests also include checking the serviceability limit state (accelerations) and increased fatigue from dynamic excitation, see e.g. [2].

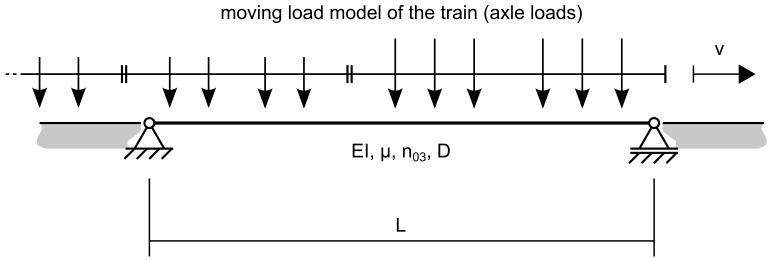

Figure 1: Moving load model (single forces representing wheelset loads of the train) on bridge model (here: simply supported beam): v traveling velocity of the train, EI bending stiffness of the bridge superstructure, μ distributed mass of the bridge superstructure, n_{03} calculated first eigenfrequency (bending) of the bridge superstructure, D damping ratio of the bridge construction, L span length.

The dynamic compatibility assessment (Germany) is divided into 5 levels, which are characterized by an increase in the level of detail (LoD) and the model complexity of the individual system components (train and bridge), see Fig. 2. The individual levels are presented and explained in detail in [1]. Current further developments of Level 2 were recently presented in [3]. In Level 2, the dynamic compatibility tests of train-bridge interaction are performed as part of a parameter study on a generic set of single-span girder bridges (simply supported beams) of span lengths from $1\,\mathrm{m}$ to $120\,\mathrm{m}$. The parameter study is based on conservative assumptions (eigenfrequency per span length and standard damping) with respect to the existing bridge stock of the railway network. In the higher Levels 3, 4 and 5, individual existing bridge structures are modeled for specific lines and their structural dynamic response is simulated when trains pass over them. In Level 3, available plan data of the individual bridge structures of a line are used for this purpose. In Level 4, the bridge model is enriched and calibrated using dynamic structural measurements (in-situ). The objective quantities of the structural measurements are the experimental identification of the existing natural frequencies and the existing applicable damping in the form of the derived damping ratio D (viscous damping model within the framework of modal consideration, linear system behavior). In Level 5, train-bridge tests are also carried out with the real test object (vehicle/train) on the bridge structure under investigation with previously identified, expected significant dynamic structural response. The investigations in Levels 3, 4 and 5 are to be carried out on a line-specific basis by evaluating a large number of structures. Hence, network-wide measurement data is available from previous investigations (e.g. from Level 4) on these individual structures. The measurement data will be characterized in more detail in the following section.

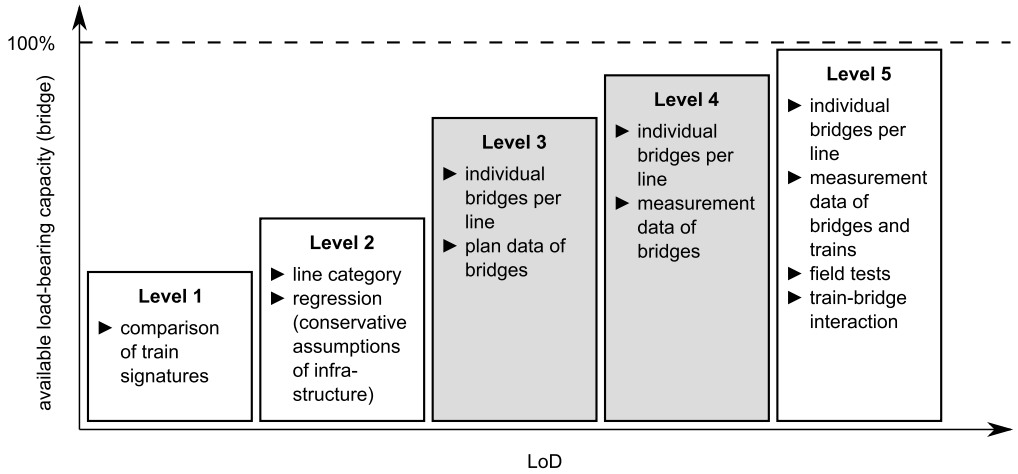

Figure 2: Levels of verification (see [1, 3]) shown as a function of the levels of detail (LoD) and potential system reserves (load-bearing capacity) for the technical network access process (DB InfraGO AG, Germany).

1.1 Problem description

In Level 3 (Fig. 2), the conservative damping (damping ratio D_{norm}) specified in DIN EN 1991-2:2010, which is employed for new structures in the planning phase, is used for the assessment of individual bridge structures. For existing bridges (railway network), there are currently no recommendations in Germany for assumptions that deviate from these values. However, in a large number of structural dynamic measurements (Level 4) carried out (see Sec. 2), it was shown that the damping values measured in existing structures are above the conservative damping values of DIN EN 1991-2:2010 in most of the cases. An initial evaluation comparing standard normative and measured values for the railway network of DB InfraGO AG (Germany) was shown in [3]. In the following, a methodology will be presented which allows to predict, i.e. reliably estimate, realistic damping values for a given bridge superstructure by relating existing damping data of bridge structures (database of measured values) and structural properties of existing bridge structures that show similar/comparable system features.

The methodology has already been successfully derived for the prediction of eigenfrequencies of existing railway bridges [4]. The present contribution presents and discusses the further development of the methodology for the prediction of damping. Note that in the following, the focus is on the processing of already available damping ratios (data) instead of their identification from experimental measurement data (i.e. acceleration-time signals).

1.2 State of the art

The correct determination of the dynamic structural damping properties is particularly relevant for the dynamic excitation of railway bridges under high-speed traffic in order to be able to realistically represent the dynamic structural response from periodic excitation, see e.g. [5, 6, 7, 8].

Data-driven machine learning (ML) approaches have been used in the field of civil engineering for a number of years, and recently with an increasing trend. In [9], for example, amplitude-dependent structural damping of buildings is mapped on the basis of building measurements using artificial neural networks (ANN) of different architectures. In addition to the application on the structural scale (e.g. [10]), ANN are also increasingly used to model/represent material behavior as an alternative for complex physically-based material models, see e.g. [11] for the derivation of damping properties of solids from their system parameters or [12] for the

specification of dynamic properties of soils (damping ratio).

In addition to extensive analytical approaches for determining the damping coefficient from the measurement signal of mostly acceleration sensors, which are installed directly on the structure and record its structural response as a result of train passage, methods have recently been developed to determine the structural properties of bridges by indirect measurement from the vehicle (during train passage). In [13], the idea of indirect measurement is described for the identification of bridge eigenfrequencies from on-vehicle acceleration sensor measurements during train passage of a bridge using a supervised deep learning-based approach with transfer learning.

In [4], an ML-based algorithm for the prediction of eigenfrequencies of railway bridges has already been presented. In the following, this approach is adopted and further developed for the available damping data [3]. For the German railway network, the functional dependence of the damping ratio for different bridge material types was already shown in [3] as a function of the span (resonant) length L (sole input variable) using linear regression.

1.3 Outline

In the following, Sec. 2 first presents the database of measured damping values for the German railway network (DB InfraGO AG) and explains the available, associated structural properties of the measured bridges. In Sec. 3, approaches for realistically predicting damping of existing bridge structures are presented. In Sec. 4, results from the different approaches are compared with each other and tested for suitability for their application. Finally, further upcoming development steps and the key findings are summarized in Sec. 6 and Sec. 7.

2 OVERVIEW OF DATA

2.1 Data basis

As a data basis for the railway network of DB InfraGO AG (Germany), series of measurements (acceleration measurements of bridge superstructures during train passage) were carried out in the past on a total of 716 bridge superstructures, see Fig. 3, of various material types (reinforced concrete / filler beam: 192, pre-stressed concrete: 116, steel/composite: 408) and the respective damping factor was determined from the acceleration signal in the decay phase of the superstructure (train has left the bridge, no additional damping induced by the train-bridge interaction). For each bridge measurement, the individual measurement results of all train passages that could be evaluated per bridge are also available. Most frequently, individual measurements from 10 train passages per bridge superstructure were recorded within such a measurement series of a bridge, see Fig. 4. The evaluation of the different train passages per measurement series already results in a distribution (scattering) of the damping ratio of the bridge superstructure under investigation (Fig. 3). In Fig. 3, the calculated (discrete) values for the 5%-fractile value, the average value and the 95%-fractile value of the damping ratio D (free decay phase) are also shown in the histogram of the individual results of such a measurement series of a bridge superstructure.

For the data basis at European level and the EU-wide bridge stock, it is referred to Sec. 6.

Most of the measurements were carried out and evaluated by DB's own system service provider and are therefore comparable to a large extent. This is a basic condition for the further evaluation of the measurement results in order to make predictions from a comparably determined data basis (damping values) and to exclude systematic errors due to different determination of individual damping values via different evaluation procedures. Acceleration

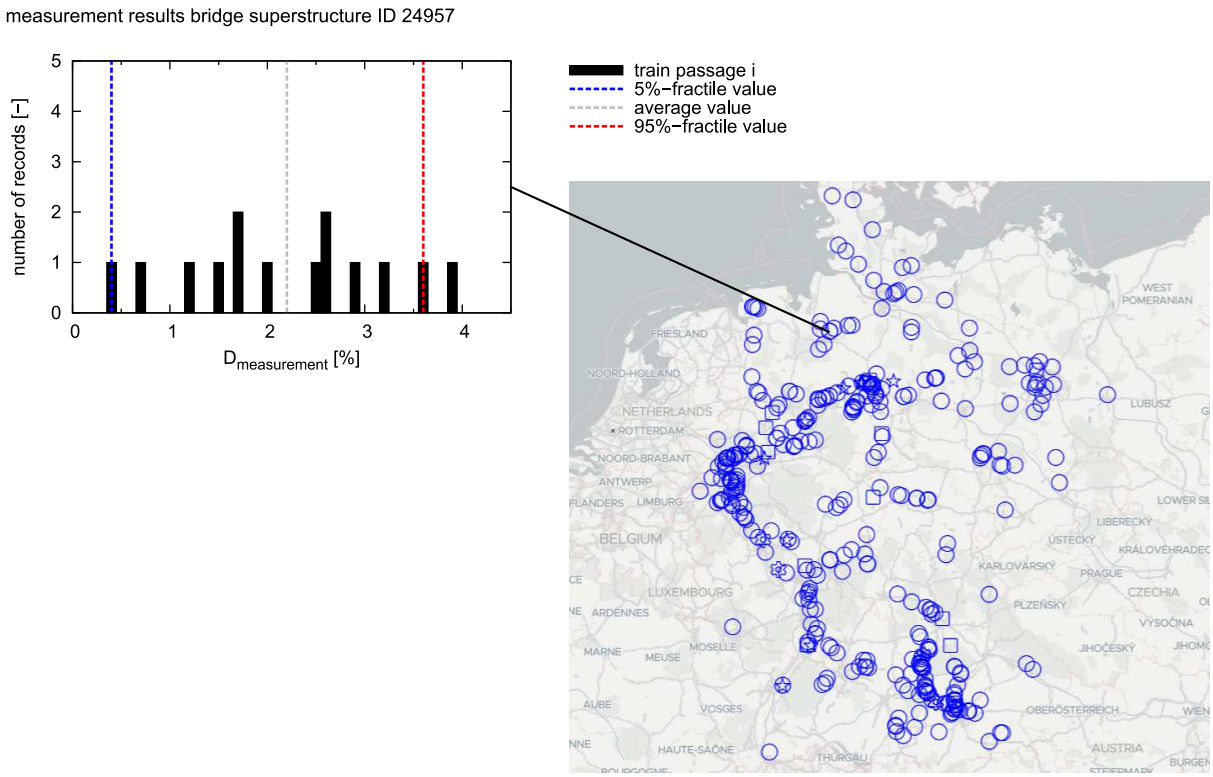

Figure 3: Map of dynamically assessed (measured) railway bridge superstructures (Germany) and example of distribution (histogram) of the identified damping ratios D (decay phase) per train passage (measurement series (example) of one bridge superstructure).

measurements (acceleration-time signals) were recorded for each dynamically measured bridge superstructure (mostly single-span girders and continuous girder systems, see Fig. 5, of national line category D4DB) using several acceleration sensors (mostly three) per bridge superstructure.

The damping ratio for each train passage was determined from the time curve of the acceleration signals of the measuring sensors (acceleration-time curve) of the decay phase (train has left the bridge), see Fig. 6 as an example, with the acceleration amplitudes $a_z(t_1)$ and $a_z(t_2 = t_1 + j\,T_d)$ separated by a time difference of j oscillation periods T_d.

The bridges were mostly selected on the basis of their dynamic significance regarding train-bridge excitation (Level 4) by high-speed traffic. In some cases, measurements were also carried out as part of structural reanalysis, e.g. for local speed increases (infrastructure velocity) in the railway network.

The data scatter recognizable in the histogram shown in Fig. 3 stems, among other things, from different boundary conditions of the measurements carried out, as different trains with different velocities were used for the acceleration recordings. It is therefore difficult to apply a probabilistic evaluation with a predefined distribution function, e.g. as described in DIN EN 1990:2021-10 Annex D (informative). The scatter will be significantly smaller under similar boundary conditions, which has also been demonstrated in the past in the context of controlled forced excitations with approximately the same boundary conditions (so-called forced oscillation, exciter or shaker measurements, see e.g. [8, 14]). In general, a further (non-linear) increase in the total damping (amplitude and speed dependence of damping features, train-bridge interaction with damping from the train chassis, non-linear structural properties) can be expected, especially in the resonance case, even if these non-linear effects are to be limited for reasons of serviceability and low fatigue. It can therefore be assumed that the use of the damping

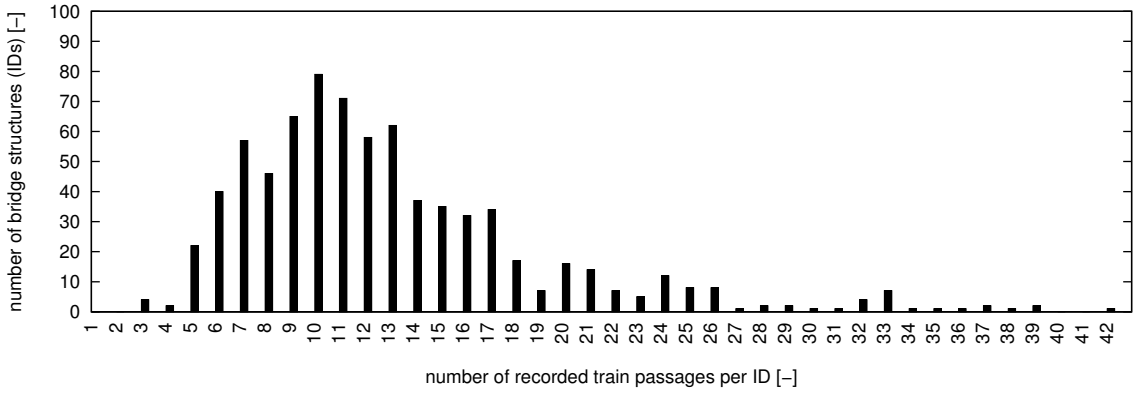

Figure 4: Overview of available data from measurement series on railway bridge superstructures: Recorded number of train passages per measurement campaign.

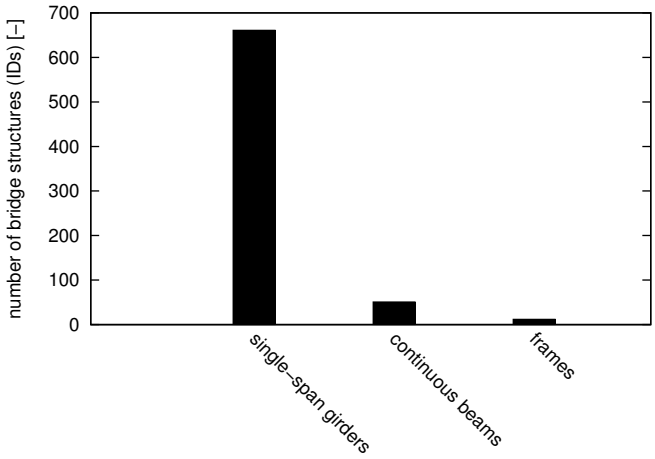

Figure 5: Overview of assessed bridge types (construction forms) with damping measurements for training.

values determined during the decay phase is probably on the safe side for application within train-bridge compatibility tests.

2.2 Measurement data and data management

As an overview of all measurements, the derived normalized results (5%-fractile, average value and 95%-fractile value of the damping ratio) are shown in Figs. 7 and 8 as a function of the material type and the span L of the bridge superstructure. The respective standard damping according to DIN EN 1991-2:2010 was used for normalization of the identified damping ratios of the measurments. Consequently, Figs. 7 and 8 show magnification factors for the expected damping ratio of existing railway bridges (DB InfraGO AG, Germany) in relation to the conservative standard damping given in DIN EN 1991-2:2010 (without additional damping from train-bridge interaction).

The linear trend functions (linear regression) plotted in Figs. 7 and 8 show the general (linear trend) of the magnification factor of the normative standard damping ratio D_{norm} (damping according to DIN EN 1991-2:2010) as a function of the span length L of the bridge superstructure. In addition to the linear regression line, other ansatz functions can also be used for the regression (polynomial regression) if sufficient data is available. However, this representation only allows an estimation of the magnification factor for the input variable L (span length) of

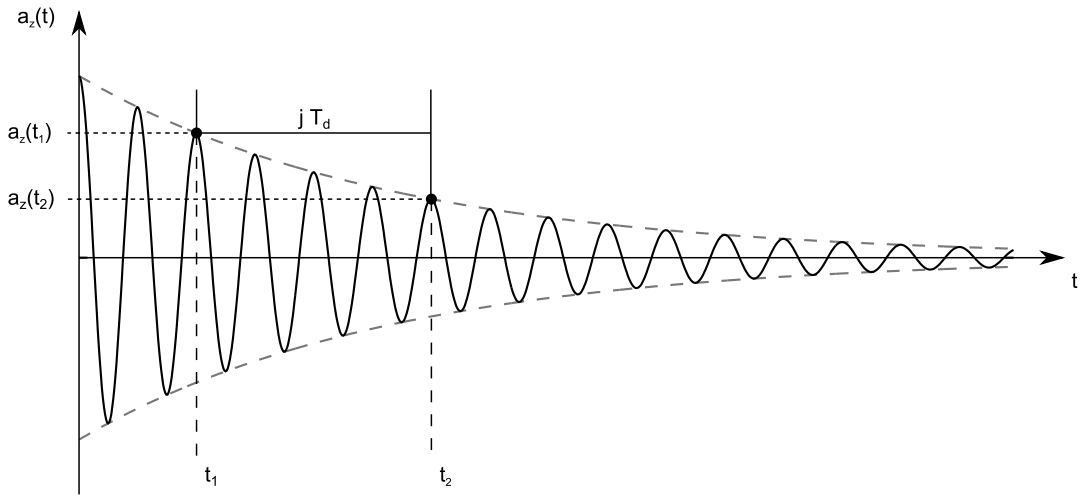

Figure 6: Idealization of the decay phase of the bridge superstructure after train passage (acceleration-time curve): Identification of the decay curve (envelope).

the bridge superstructure. The influence of other input variables (structural properties) for a given span length L is not identifiable in this case. A more realistic and more reliable damping prediction is possible with an available database by comparing/including several structural properties (influencing input variables). Two approaches are discussed in Sec. 3.

The damping ratio obtained from measurement (Level 4) of the bridge superstructures was stored in a database (digital model of the railway bridge stock, see [1]). Each bridge superstructure is assigned a dataset which, in addition to the measured damping ratio, also contains other structural properties from plan data or other data sources (e.g. traffic data, timetable data) after data fusion. Data fusion enables in the following to correlate individual structural properties with the measurement data and to specify influencing variables from the comparison across the entire measured railway bridge stock.

2.3 Sources of damping and influencing variables

Sources of damping (Fig. 9) can be assigned to one of the three main groups, i.e.

- material damping (building material),
- structural damping (connections),
- geometrical damping (radiation damping),

see also [15]. While material damping originates from local material properties and its dissipative behavior due to applied time-dependent and recurring (cyclical) loading and unloading, structural damping at the macroscale includes constructive structural properties for further damping contributions (e.g. from the presence of relative friction from ballast [7, 16]), dissipative relative motion of structural parts (component connections) or built-in technical damping components. For dynamic problems, the system boundaries must be described even more realistically in detail than in static calculations in order to correctly capture the interaction with the environment (subsoil). Above the cut-off frequency of the respective soil system, waves propagate into the surrounding subsoil and thus cause a geometrically induced energy transport away from the vibration source. In addition to the shape of the abutments and the dynamic (usually non-linear) bedding properties (decisive for frames), the geometry and the environment (soil

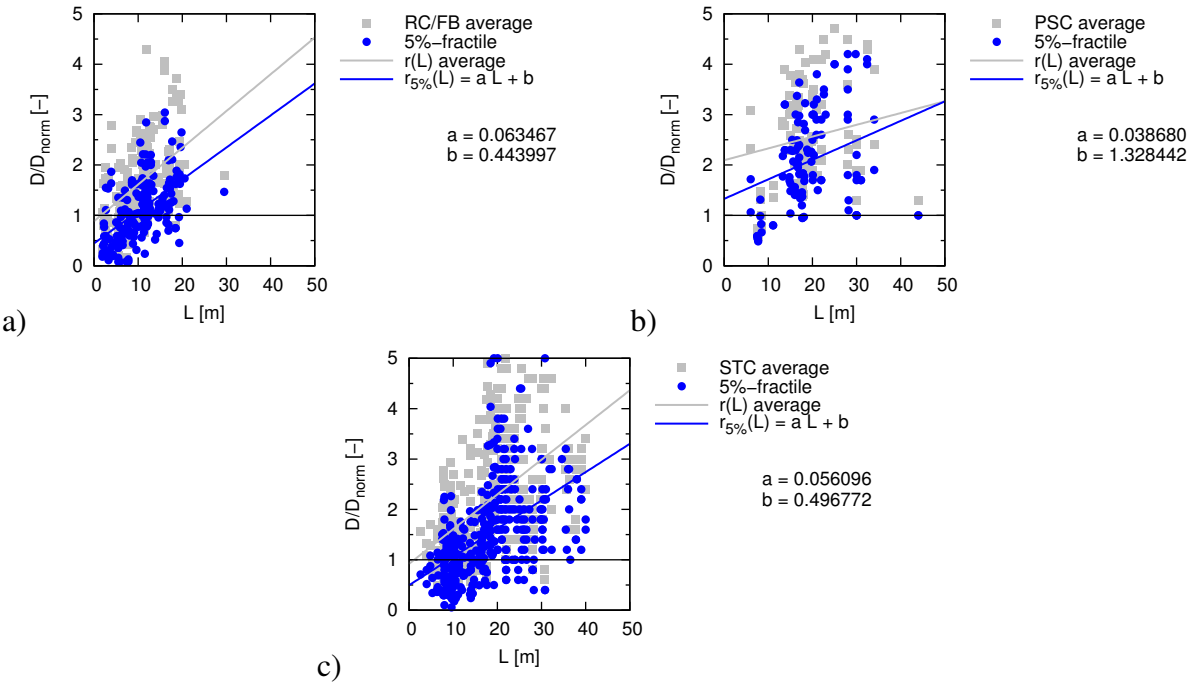

Figure 7: Magnification factor of standard damping ratio (average value and 5%-fractile value) resulting from measurement series of different railway bridge superstructures with span length L (DB InfraGO AG, Germany): a) RC/FB – reinforced concrete / filler beam, b) PSC – pre-stressed concrete, c) STC – steel/composite.

properties) of the subsoil also play a role, see e.g. [17, 18]. The experimental measurement usually includes different dominant proportions of the individual sources. The mathematical identification of individual proportions (example ballast: [7]) is usually challenging [19, 20]. While detailed information on the material, construction type and other structural properties of the individual bridge superstructures is generally available from plan data in the database, the geotechnical characteristics of the surrounding soil are less detailed and represent a source of data uncertainty. For this reason, their influence is not discussed further in the following and it is assumed that they play a subordinate role compared to material and structural damping. Figure 9 illustrates the different sources of damping and possible geometrical and structural building properties (influencing variables).

The general functional representation of the damping value per material type and span length L as only influencing input variable is limited due to the significant variance and uncertain correlation. In addition, damping values evaluated by measurement are subject to a high degree of uncertainty. In the standard DIN EN 1991-2:2010, conservative assumptions (lower limit of previously evaluated damping values of reference bridges) are specified for each material type and span length L. These assumptions therefore provide very conservative values for damping ratios without taking other influencing variables into account for the same span length L. Dynamic structural responses calculated with these values generally provide excessively large calculated vibration amplitudes when trains pass, which can still be considered an advantage when designing new structures for later system reserves. In the case of existing structures that can no longer be modified by design, however, the overestimated dynamic structural responses usually lead to verification problems when new train types are introduced (technical network access process with dynamic train-bridge compatibility checks). A further consequence consists in an underestimated residual load-bearing capacity in the context of fatigue investigations, which should be avoided in the interests of efficient resource-conserving management of rail-

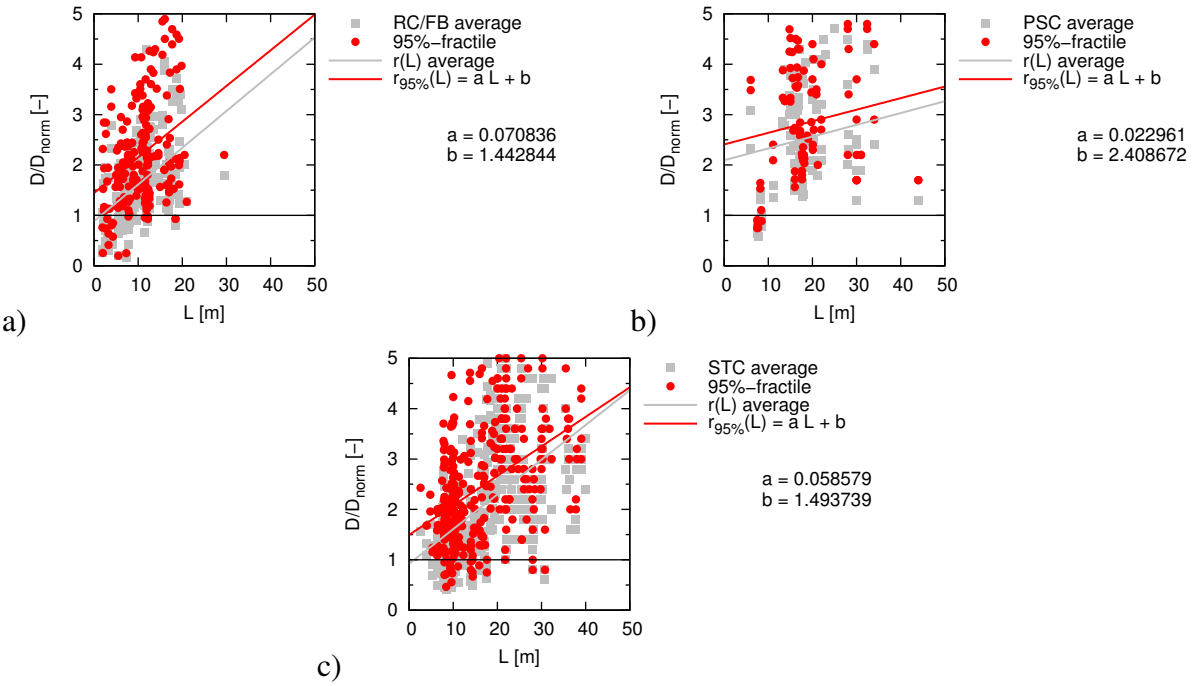

Figure 8: Magnification factor of standard damping ratio (average value and 95%-fractile value) resulting from measurement series of different railway bridge superstructures with span length L (DB InfraGO AG, Germany): a) RC/FB – reinforced concrete / filler beam, b) PSC – pre-stressed concrete, c) STC – steel/composite.

way infrastructure. Previous investigations and attempts at quantification [21, 22] (prediction of more realistic, mathematical damping values from energy considerations of dissipation of the individual bridge components, ballasted superstructure separate from the remaining construction on a simple Euler-Bernoulli beam model) have shown that the design of the bearing of the rails (superstructure: ballast or slab track, rails longitudinally movable or fixed) have a significant influence on the existing damping values. In general, it can be stated that the presence of slab tracks leads to small values, sleepers in ballast lead to higher damping values of the overall structure due to relative movements in the ballast bed (mainly with high-frequency vibration) or additional friction at system boundaries and a better load distribution (more favorable, i.e. lower, dynamic excitation). In addition to the design of connection details, an influence from the year of construction can be expected. Older structures generally exhibit greater wear with associated increased dissipative properties due to structural damping contributions. In the case of reinforced concrete and pre-stressed concrete structures, older structures may have entered state II (cracked state of the concrete tension zones), while in the case of steel bridges, increased friction occurs mainly at structural connections (joints, connection details). In addition to the influencing quantities mentioned, the general design of the static load-bearing system (single-span girders, continuous girders, frames, special structures: e.g. tied-arch bridges) also has group-related properties, i.e. a combined consideration can also lead to strongly varying damping properties for the same remaining system parameters. With extensive data, it is therefore promising to compare structures with as many similar system parameters as possible (taking into account a relative tolerance for each influencing variable if necessary). The system parameters examined in the following as input variables are described in Sec. 3.

The existing database (DB InfraGO AG, Germany) does not currently have a sufficient scope to provide several datasets (results from measurements) for every possible set of different influencing variables. In this case, the approach of larger relative tolerances per influencing variable

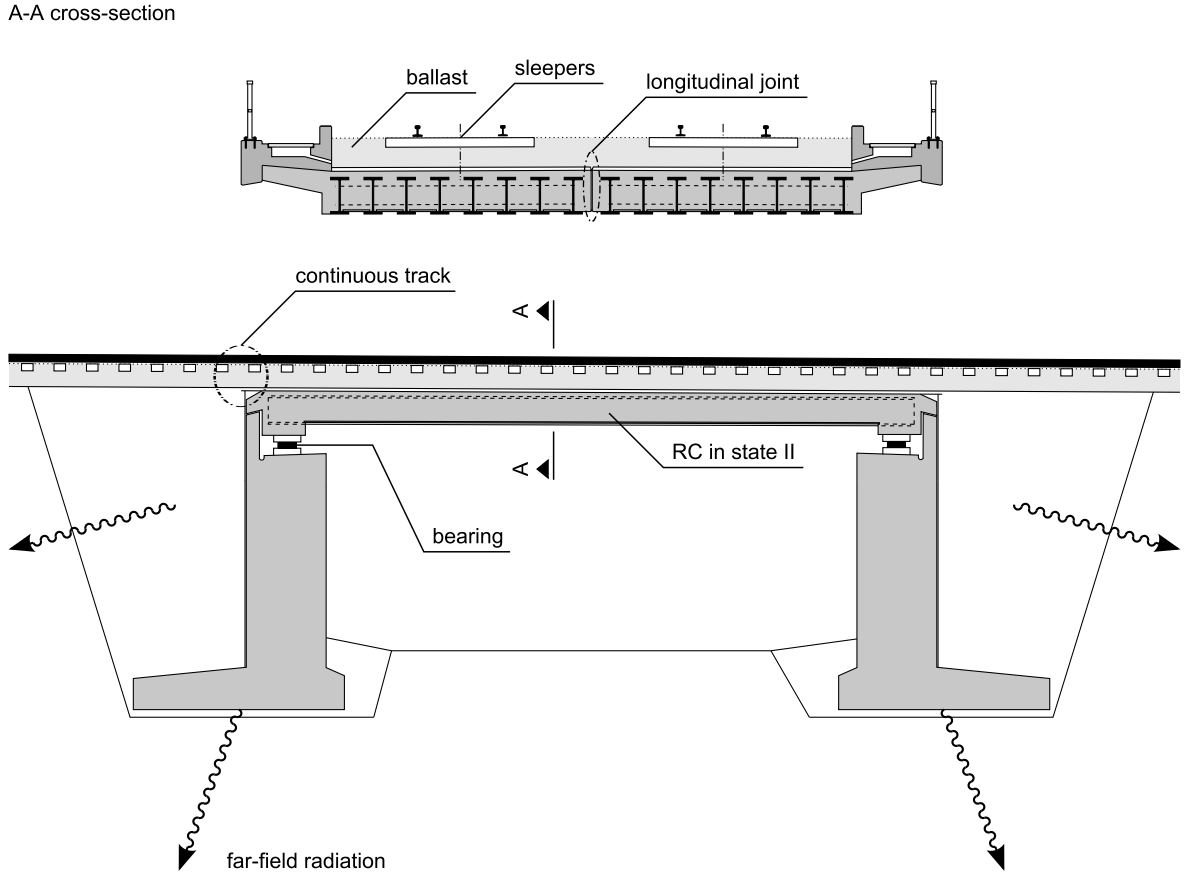

Figure 9: Sources of damping: schematic illustration for the case of a simply supported railway bridge superstructure.

can be expedient for a selection of system-related similar structures. In addition, even almost identical bridge superstructures (e.g. arranged in parallel as part of an overall double-track bridge structure) sometimes show significant deviations in the damping value determined by measurement, which can indicate other influencing variables (e.g. excitation by train passage).

3 METHODS FOR DAMPING PREDICTION

In recent years, ML methods have also been increasingly used in civil engineering. Figure 10 provides an overview of ML approaches by highlighting the selected ones studied in the following. The strength of data-based ML approaches is based on the model-free assessment of available data. For the prediction of objective quantities, no physical relationships need to be captured a priori by means of an analytical or physically based model as an initial assumption. ML relates a large number of influencing variables (input data) to objective quantities. In the present case, the following input variables per bridge superstructure are selected:

- span length L,
- line speed v_{infra} on the bridge superstructure,
- bending stiffness EI of bridge superstructure,
- year of construction,
- distributed mass μ of bridge superstructure,

- calculated first bending eigenfrequency n_{03} (Level 3),
- track type,
- type of static system.

The bridge measurements listed in Sec. 2 (with individual measurement results for each train passage) are available as the data basis for regression and training in case of ML: reinforced concrete / filler beam (RC/FB): 192, pre-stressed concrete (PSC): 116, steel/composite (STC): 408. In addition, further measurement results from earlier measurement campaigns are available only including objective quantities (average damping ratio of the measurement series per bridge superstructure). These additional datasets are used in the following for validation for regression and ML approaches: reinforced concrete / filler beam (RC/FB): 107, pre-stressed concrete (PSC): 19, steel/composite (STC): 40.

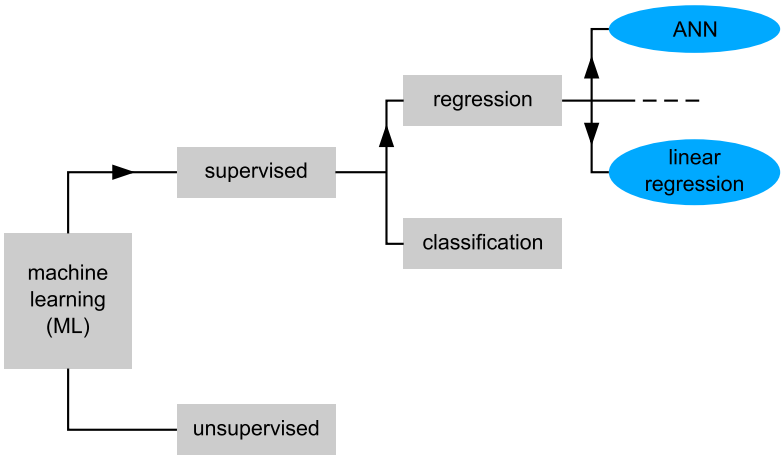

Figure 10: Overview of ML approaches.

3.1 Linear interpolation and regression approach

The linear multidimensional (n-dimensional) regression (MR) approach is based on the search for interpolation points that originate from existing measurement data (average values) and structural properties, see Fig. 11. For the prediction of damping features of bridge structures, a database query is executed in which relevant similar structures are identified via their structural properties (n-dimensional in general, here $n = 8$) and compared to the query object with a possible tolerance of the deviation (degree of similarity). For continuous variables (e.g. bending stiffness EI, distributed mass μ, span length L), the objective quantity is (linearly) interpolated from existing measurements for the query. No interpolation takes place for discrete input variables (e.g. construction type, material type, track type); here only similar bridge superstructures are included in the list of results. The process is shown in algorithmic form in Alg. 1.

The existing database does not have a regular grid (grid points) that would enable regular interpolation. For this purpose, three (intermediate) objective quantities are determined from a cluster of identified similar bridge superstructures evaluated by measurement: predicted minimum value, predicted average value for several datasets, predicted maximum value. The interpolation procedure for this data triple is illustrated in Fig. 11.

Algorithm 1 Computation sequence: n-dimensional interpolation.

► initialize damping array $\mathbf{D} = \mathbf{0}$
► read in system parameters of existing bridge from input file: n ident_parameters
► normalization of the system parameters of existing bridges
for all bridge IDs i in database **do**
  if $D_i > 0$ (damping measurement results are available for bridge i) **then**
    for system parameter j of n **do**
      if abs (parameter(i, j) − ident_parameter(j)) $\leq$ tol(j) **then**
        ► add D_i to array $\mathbf{D}$
      end if
    end for
  end if
end for
► compute minimum of $\mathbf{D}$
► compute average of $\mathbf{D}$
► compute maximum of $\mathbf{D}$
► compute damping limits D_{norm}
► post-processing: output $D_{\text{pred}/D_{\text{norm}}}$

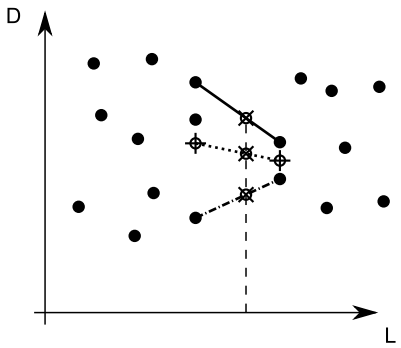

Figure 11: Interpolation with range formed by minimum, average and maximum predicted value.

3.2 Machine learning: Artificial neural network

In addition to the approach presented in Sec. 3.1, several ANN architectures were used to predict the damping values and their suitability was tested after training and validation. The following steps are required for the application of an ANN:

- training,
- validation,
- testing.

The selected architectural and training parameters of the ANN are listed in Tab. 1. According to an expert approach, a separate ANN (A1, A2, A3) is formulated and trained for each bridge material type (A1: RC/FB, A2: PSC, A3: STC) using the average values of damping measurements, see Figs. 7 and 8. A multi-layer feed-forward network is used as basic network architecture, see Fig. 12 for each ANN. A backward-forward training algorithm (stochastic gradient descent (SGD) optimization) is employed during the training phase. Various ANN architectures and parameter combinations were tested for the selection of the final ANN architectures and the training parameters. The final parameters are shown in Tab. 1.

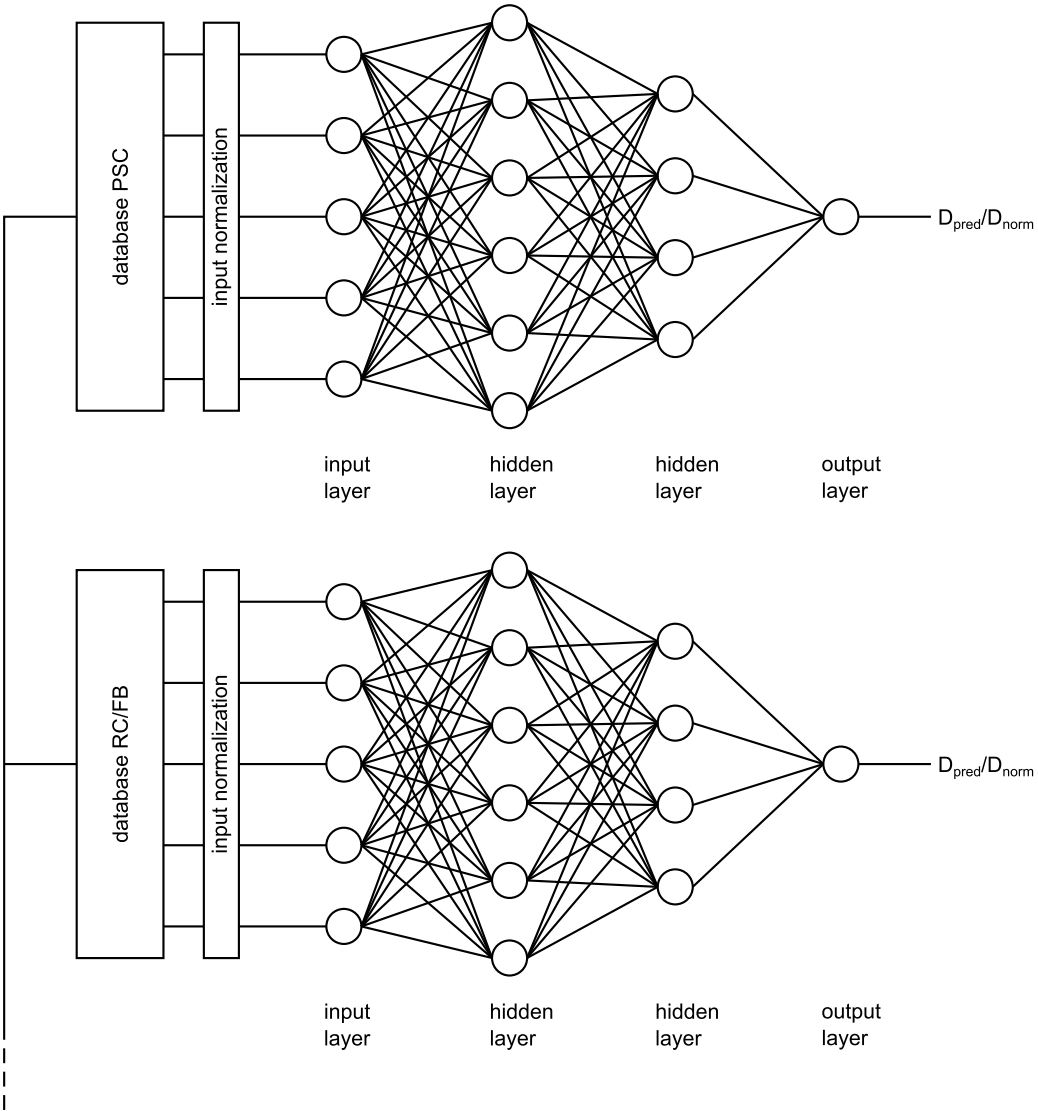

Figure 12: ANN architecture (schematic illustration) multi-layer feed-forward network for bridge material types RC/FB (A1), PSC (A2) and STC (A3).

Fig. 13 shows the computed root mean square error (RMSE), i.e.

$$\text{RMSE} = \sqrt{\frac{1}{m}\sum_{i=1}^{m}\left(\frac{D_{\text{pred},i} - D_i}{D_{\text{norm},i}}\right)^2}, \tag{1}$$

for the training of the different ANN (A1, A2, A3) for the bridge material types RC/FB, PSC and STC. The algorithmic sequence for a query using ANN is specified in Alg. 2.

4 COMPARISON OF RESULTS AND DISCUSSION

This section presents the results from the two previously presented approaches for predicting the damping properties in terms of the magnification factor

$$V_D = \frac{D_{\text{pred}}}{D_{\text{norm}}} \tag{2}$$

network architecture:	**A1**: RC/FB	**A2**: PSC	**A3**: STC
number of input neurons	8	8	8
number of hidden layers	3	3	3
number of neurons per hidden layer	48-32-16	48-32-16	48-32-16
type of transfer function per hidden layer	tanh-linear-linear	tanh-linear-linear	tanh-linear-linear
batch size	100	100	100
number of epochs	1000	1000	1000
training size	192	116	408
test size	107	19	40
learning rate	0.001	0.001	0.001
decay rate	0.9	0.9	0.9
β_1	0.85	0.85	0.85
β_2	0.95	0.95	0.95
ε	$1.0 \cdot 10^{-8}$	$1.0 \cdot 10^{-8}$	$1.0 \cdot 10^{-8}$

Table 1: Training parameters for selected artificial neural networks A1, A2, A3.

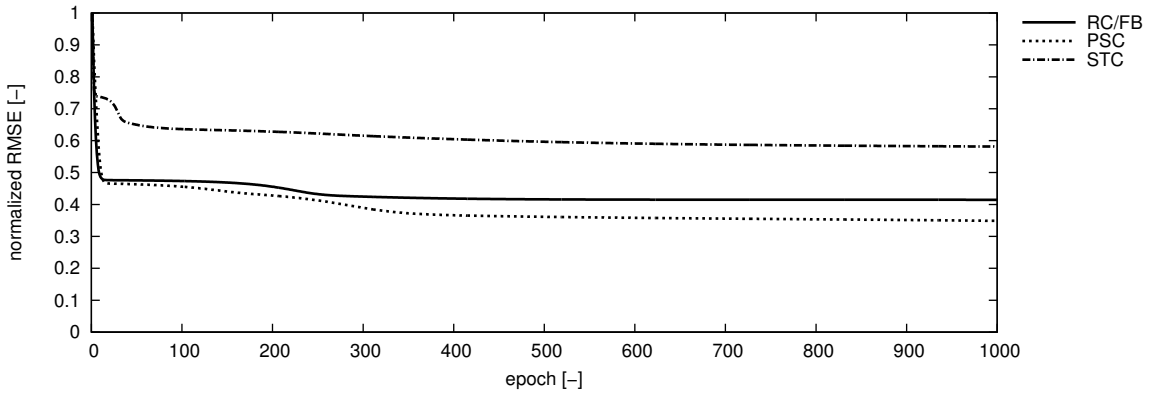

Figure 13: Root mean square error (RMSE) during training.

of the standard damping ratio (DIN EN 1991-2:2010) for selected examples. In Sec. 4.1, the quality of the prediction is first shown using other available bridge measurements (test cases) that were not previously included in the prediction approaches. In Sec. 4.2, sensitivity studies are carried out on selected examples to highlight the dependence of the objective quantity on the input variables.

4.1 Testing

In the following, measurement data from other, additional bridge measurements not previously included in the training and validation phase are compared with the predicted damping values in terms of the magnification factor of the standard damping ratio, see Fig. 14. The comparison of the measured and predicted damping values in Fig. 14 still shows a significant scattering. This is due to the small amount of available training data and other system parameters not yet included in the study, which will have a specific and system-related influence on the damping to be expected in reality. In general, the prediction of damping values can be expected to have a higher scattering and, consequently, a greater uncertainty than compared to the eigen-

Algorithm 2 Computation sequence: ANN

► initialize ANN architecture A1, A2 or A3
► initialize training dataset from database
for all bridge IDs i in database **do**
  if $D_i > 0$ (damping measurement results are available for bridge i) **then**
    ► use normalized dataset i for training and validation with n system parameters (features) and normalized objective quantity $D_i/D_{\text{norm},i}$
  end if
end for
► read in system parameters of existing bridge superstructure from input file: n ident_parameters
► call ANN prediction for system parameters: n ident_parameters
► output $D_{\text{pred}}/D_{\text{norm}}$

frequency, see investigation presented in [4]. The strength of an application of ML methods is only achieved if a sufficiently large database is available. Nevertheless, the predicted damping magnification factors are predominantly below those of the magnification values achieved from measurements, see Fig. 14, which leads to a statement on the safe side. For further safety considerations in the case of an application in a safety-relevant context, it is referred to Sec. 5.

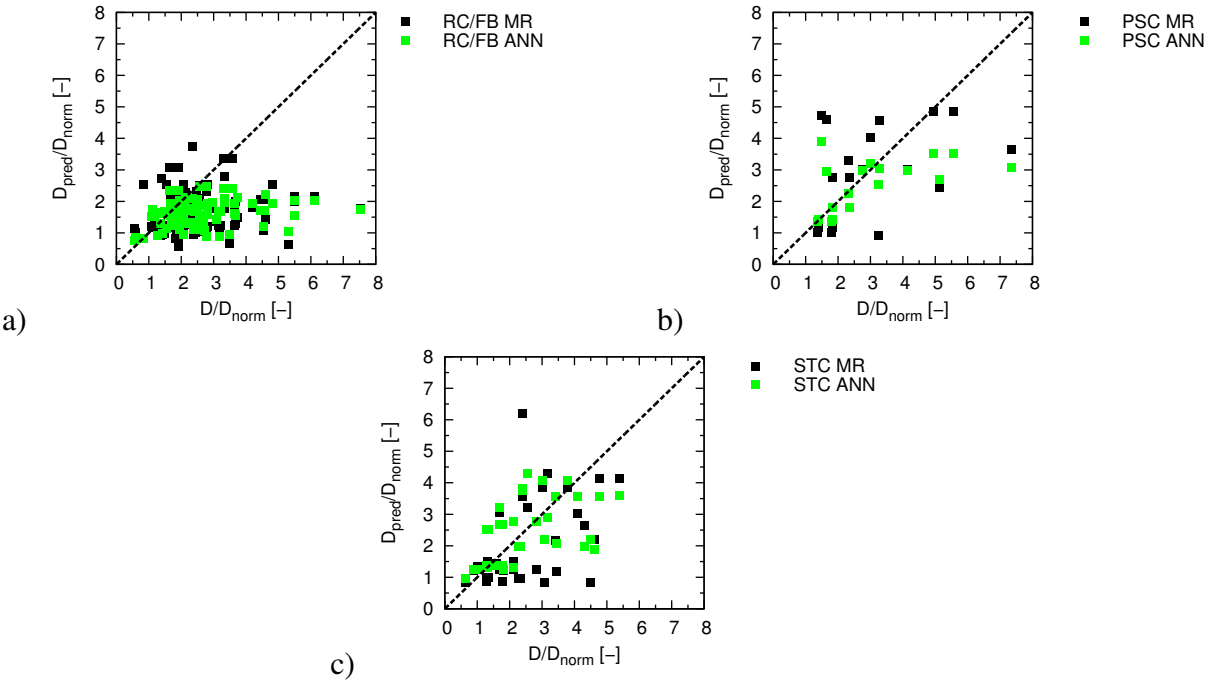

Figure 14: Comparison of measurement results in terms of D/D_{norm} and predicted results in terms of $D_{\text{pred}}/D_{\text{norm}}$ obtained from MR and ANN: a) RC/FB – reinforced concrete / filler beam, b) PSC – pre-stressed concrete, c) STC – steel/composite.

4.2 Application: Sensitivity of damping ratio with respect to input variables

As an application case, the prediction of the damping magnification factor for fixed structural properties but varying span length L is investigated. Figure 15 shows the results for the bridge superstructures RC/FB, PSC and STC. In the case of MR, a prediction range consisting of minimum, average and maximum values is obtained.

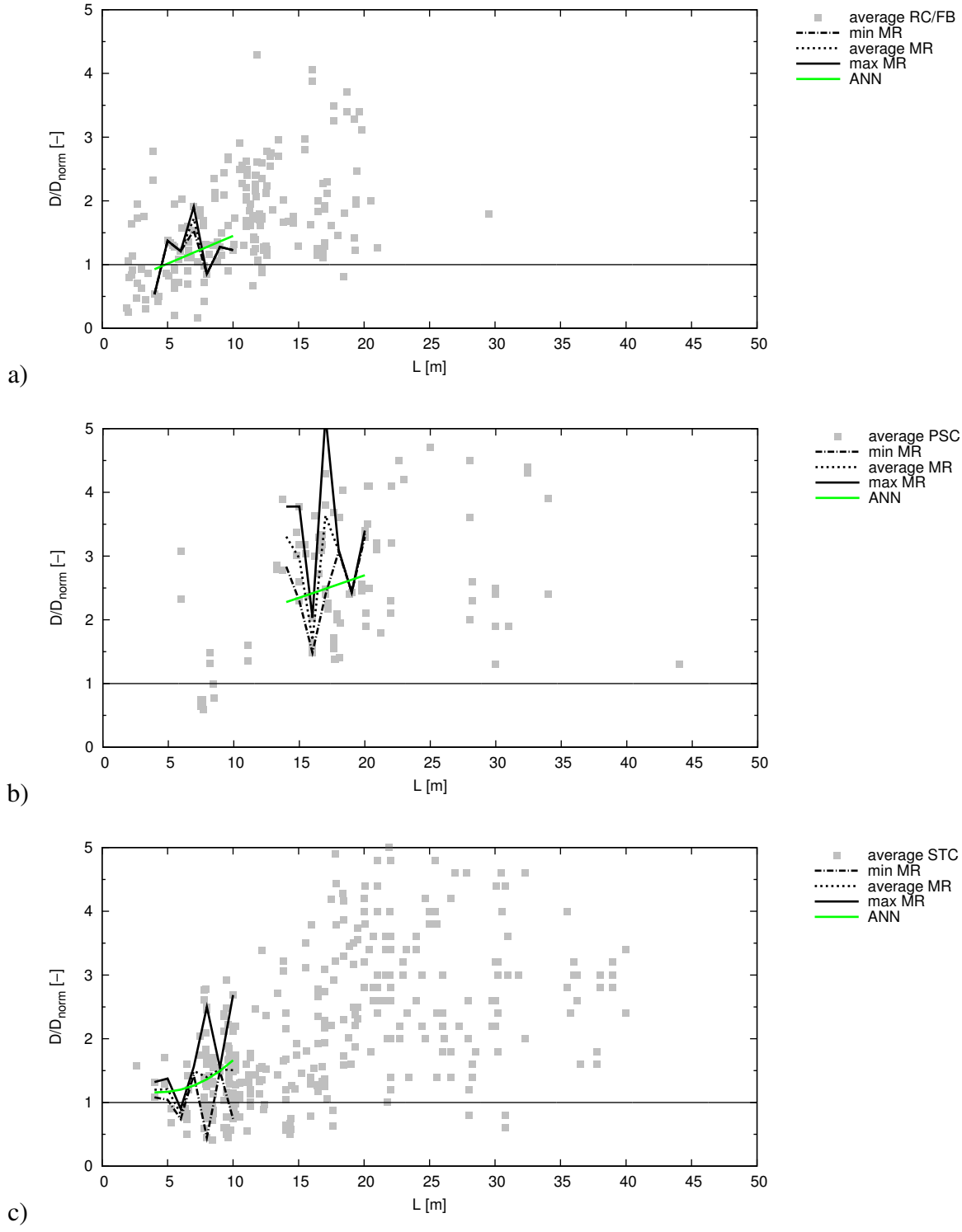

Figure 15: Predicted damping magnification factor $D_{\text{pred}}/D_{\text{norm}}$ for a fixed set of input parameters but varying span length L (available normalized average measurement values (training set) plotted in grey): a) RC/FB – reinforced concrete / filler beam (example: $4\,\text{m} \leq L \leq 10\,\text{m}$), b) PSC – pre-stressed concrete (example: $14\,\text{m} \leq L \leq 20\,\text{m}$), c) STC – steel/composite (example: $4\,\text{m} \leq L \leq 10\,\text{m}$).

It can be seen that the magnification factors depend heavily on the set of input variables and cannot be specified solely as a function of the span length L. The results from the ANN approach are largely in the range formed by the minimum and maximum values from the MR results.

Figures 16 and 17 show results for parameter studies of randomly selected bridge superstructures (ex. 1 to 3, respectively) using the ANN approach for different input variables (year of construction, line speed, presence of sleepers and ballast, construction type) with further input variables for predicting the damping magnification factor.

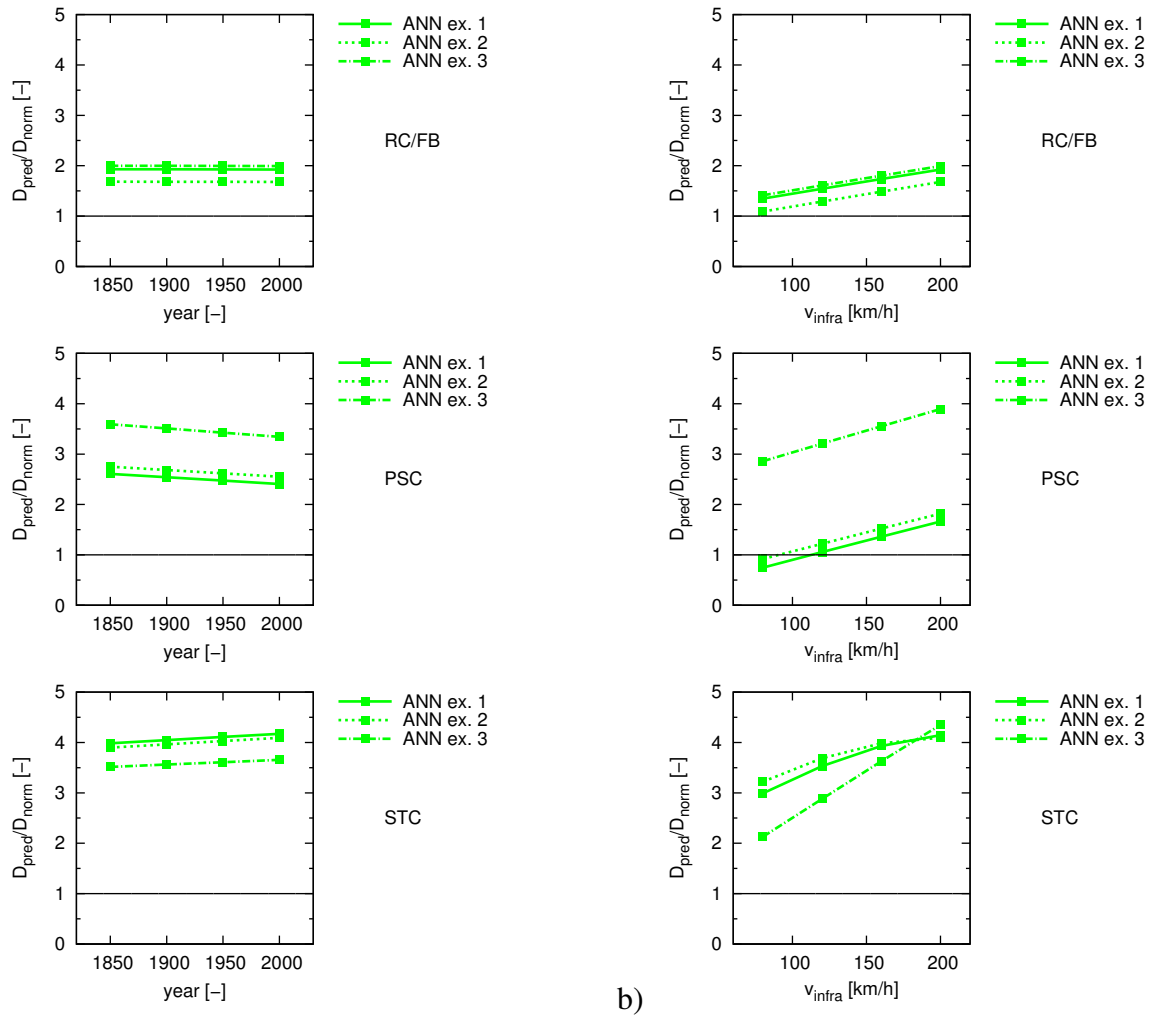

Figure 16: Sensitivity as a function of the input variables (features) for selected bridge examples (other input variables fixed): a) year of construction, b) line speed v_{infra} on the bridge superstructure.

From these exemplary results for selected individual examples of bridge superstructures, the assumption can be confirmed that mainly for concrete (RC/FB and PSC) higher damping magnification factors are predicted for older bridge superstructures and the values decrease for younger bridge superstructures. The influence of the line speed on the bridge superstructure (infrastructure velocity) is significant and leads to a clear increase in the predicted damping magnification factors at higher velocity. This may be due to the greater accelerations recorded during the measurements and therefore more significant damping values in the decay phase (amplitude-dependent damping). For RC/FB and PSC bridge superstructures, higher damping

magnification factors are predicted in the presence of sleepers or ballast. For STC bridge superstructures, the trend is less clear for the sample bridges examined. A clear decreasing trend of the damping magnification factors can be observed for the case of the static system of the bridges, where larger values are predicted for single-span girder systems compared to more moderate values for continuous girder systems and even low values for portal frames. However, reference should be made here to the database (Fig. 5), which contains a significantly higher number of single-span girder systems compared to continuous girder systems or portal frames that were previously measured. However, the trend could be explained by the higher acceleration amplitudes and the associated higher damping effects for single-span girder systems.

To summarize, the sources of damping previously mentioned in Sec. 2.3 can be confirmed for high damping contributions in the overall structural response.

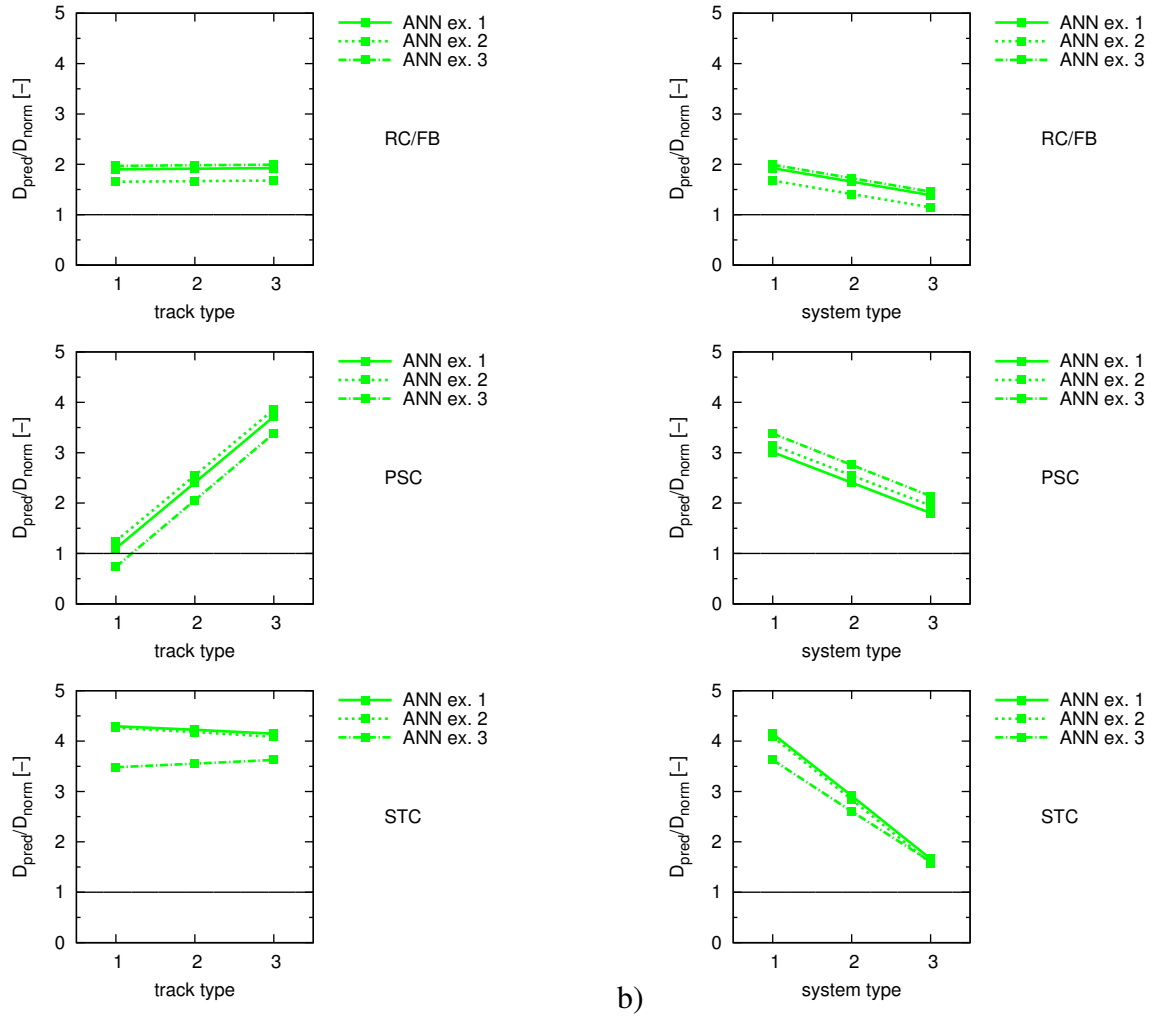

Figure 17: Sensitivity as a function of the input variables (features) for selected bridge examples (other input variables fixed): a) track type (1 = direct rail fastening / slab track, 2 = sleepers, 3 = sleepers and ballast), b) construction type (1 = singe-span girder, 2 = continuous girder, 3 = portal frame).

5 APPLICATION REQUIREMENTS

For application in the field of structural engineering verifications, further safety-relevant issues still need to be assessed and clarified as part of further research activities (see also Sec. 6).

A possible procedure is outlined in the following.

First, the input variables of the dataset used for prediction are checked whether each input variable lies within the training range (input variables within the interval of available experimentally measured and assessed bridge superstructures during training/regression). Second, physical limits are also specified for the damping magnification factor V_D. As a suggestion, for damping magnification factors greater than the value obtained from the regression line in Fig. 8 as a function of L, the value of the linear regression function (95%-fractile) is set as maximum value. In analogy, for damping magnification factors $V_D < 1$, i.e. the predicted damping ratio D_{pred} is smaller than the standard damping D_{norm} according to DIN EN 1991-2:2010, $V_D = 1$ is used or values $V_D < 1$ obtained from the regression line in Fig. 7 if the value of the linear regression function (5%-fractile) is less than 1. Third, for the use of the predicted damping values D_{pred}, a constant partial safety factor γ_D is proposed in analogy to DIN EN 1990:2021 Annex D (informative),

$$D_{\text{pred,d}} = \frac{D_{\text{pred}}}{\gamma_D} = \frac{V_D\, D_{\text{norm}}}{\gamma_D} \quad \text{e.g. with} \quad \begin{cases} \gamma_D > 1.0 & \text{for} \quad D_{\text{pred}}/D_{\text{norm}} > 1\,, \\ \gamma_D = 1.0 & \text{for} \quad D_{\text{pred}}/D_{\text{norm}} \leq 1\,, \end{cases} \tag{3}$$

see also the ansatz proposed in [4]. The design value $D_{\text{pred,d}}$ not only allows higher damping values, but also takes into account lower measured values for special steel structures in reality, see Figs. 7 and 8, in terms of predicted values $D_{\text{pred,d}} < D_{\text{norm}}$. In these cases, the standard damping ratio given in DIN EN 1991-2:2010 is higher than the damping ratio determined by measurement/prediction of the individual bridge superstructure, i.e. the predicted values are on the safe side (compared to an assessment using standard damping). Reasons for low damping ratios (measured on real structures) are currently still discussed, but may stem from insufficient structural excitation by passing trains or noise in the measurement signals due to high-frequency structural response.

The use of estimated damping values should also depend on the LoD of the model approach. It has already been shown in the past [23] that simpler models of train-bridge interaction (e.g. with fixed axle loads represented by time-constant forces) provide more conservative results compared to multi-body models of train-bridge interaction. In the latter case, predicted damping values should not be used due to lack of system reserves.

6 EXTENSION TO EUROPEAN SCALE

Within the EU research project InBridge4EU (`https://inbridge4eu.eu`), the national results (Germany) are currently compared and harmonized with the European railway bridge stock. Within the EU research project, the afore-described national bridge stock (Germany) is broadened by including other European bridges of different construction types from the countries France, Spain, Sweden and Portugal [24]. While a first goal consists in deriving harmonized European recommendations for the description of new railway bridges (conservative assumptions), the consideration of existing measured values of railway bridges in the European railway network enables a damping prediction of comparable existing bridges at the same time on the European scale (i.e. with the main focus of application on train-bridge compatibility checks).

However, it has already been shown that construction types differ from country to country and, therefore, the national features of bridge construction should be included as an input variable governing the overall damping features of the bridge types.

7 CONCLUSIONS

In this contribution, two different approaches were presented to predict damping of existing but not yet measured railway bridges by comparing them with an already measured bridge stock and similar input parameters. The damping ratio plays a decisive role in correctly assessing the dynamic train-bridge interaction and calculating the realistic dynamic structural response. It could be shown that both the application of multidimensional interpolation and an ANN trained on the basis of the available structural and damping data can be used and provide similar predicted objective quantities for magnification factors of standard damping ratios given in DIN EN 1991-2:2010. In addition to a safety margin (partial safety factor) on the predicted objective quantities, boundary conditions (limits of applicability) were also implemented to prevent unrealistically large or small objective quantities for damping values. Using a comparison of both approaches, the variation in the predicted damping magnification factor (sensitivity) due to changes in the input variables (system parameters) could be shown for selected examples. The sensitivity analysis also allows a deeper understanding of the dependence of the damping values on the structural properties.

In addition to the damping properties, the realistically determined eigenfrequency (natural frequency) plays a decisive role in the realistic calculation of the dynamic structural response of railway bridges during train passage. As shown in [4], the procedure presented in this contribution can also be employed to predict the realistic eigenfrequency of existing railway bridges.

ACKNOWLEDGEMENT

Parts of the research reported herein have been carried out within the EU research project InBridge4EU. The funding received from the Europe's Rail Joint Undertaking under Horizon Europe research and innovation program under grant agreement No. 101121765 (HORIZON-ER-JU-2022-ExplR-02) is gratefully acknowledged.

REFERENCES

[1] G. Grunert, Data and evaluation model for the description of the static-dynamic interface between trains and railway bridges. *Engineering Structures*, **262**, 114335, 2022.

[2] R. Behnke, G. Grunert, X. Liu, Bewertung der fahrzeugspezifischen Ermüdungseinwirkung auf Bestandsbrücken bei Zugüberfahrt. *18. D-A-CH-Tagung, Erdbebeningenieurwesen und Baudynamik*, September 14-15, Kiel, 2023.

[3] R. Behnke, G. Grunert, X. Liu, Level 2-calculations of dynamic vehicle-bridge compatibility for determining permissible speeds in the railway network. *9th European Congress on Computational Methods in Applied Sciences and Engineering (ECCOMAS 2024)*, Lisbon, June 3-7, 2024, DOI: 10.23967/eccomas.2024.306.

[4] G. Grunert, D. Grunert, R. Behnke, S. Schäfer, X. Liu, S.R. Challagonda, A machine learning-based algorithm for the prediction of eigenfrequencies of railway bridges. *International Journal of Structural Stability and Dynamics*, 2540016, 2024.

[5] M. Brunetti, J. Ciambella, L. Evangelista, E. Lofrano, A. Paolone, A. Vittozzi, Experimental results in damping evaluation of a high-speed railway bridge. *Procedia Engineering*, **199**, 3015–3020, 2017.

[6] A. Silva, D. Ribeiro, P.A. Montenegro, G. Ferreira, A. Andersson, A. Zangeneh, R. Karoumi, R. Calçada, New contributions for damping assessment on filler-beam railway bridges framed on In2Track EU projects. *Applied Sciences*, **13**, 2636, 2023.

[7] A. Stollwitzer, L. Bettinelli, J. Fink, Approach for the mathematical calculation of the damping factor of railway bridges with ballasted track. *IABSE Symposium: Challenges for Existing and Oncoming Structures*, Prague, May 25-27, 2022, DOI: 10.2749/prague.2022.1460.

[8] A. Stollwitzer, L. Bettinelli, J. Fink, Methods for reducing the output scatter of results for determining realistic damping factors of railway bridges. *Journal of Physics: Conference Series*, **2647**, 102005, 2024.

[9] Q.S. Li, D.K. Liu, J.Q. Fang, A.P. Jeary, C.K. Wong, Using neural networks to model and predict amplitude dependent damping in buildings. *Wind and Structures*, **2**, 25–40, 1999.

[10] Z. Chen, L. Zhang, K. Li, X. Xue, X. Zhang, B. Kim, C.Y. Li, Machine-learning prediction of aerodynamic damping for buildings and structures undergoing flow-induced vibrations. *Journal of Building Engineering*, **63**, Part A, 105374, 2023.

[11] P. Veeramuthuvel, K. Shankar, K.K. Sairajan, R. Machavaram, Prediction of particle damping parameters using RBF neural network. *Procedia Materials Science*, **5**, 335–344, 2014.

[12] W.-Q. Feng, M. Bayat, Z. Mousavi, L. Bin, A.-G. Li, J.-F. Lin, Prediction of normalized shear modulus and damping ratio for granular soils over a wide strain range using deep neural network modelling. *Georisk: Assessment and Management of Risk for Engineered Systems and Geohazards*, 2443457, 1–30, 2024.

[13] S. Lorenzen, H. Berthold, M. Rupp, L. Schmeiser, E. Apostolidi, J. Schneider, J. Brötzmann, C.-D. Thiele, U. Rüppel, Deep learning based indirect monitoring to identify bridge natural frequencies using sensors on a passing train. *11th International Conference on Bridge Maintenance, Safty and Management (IABMAS 2022)*, Barcelona, July 11-15, 2022.

[14] M. Reiterer, S. Lachinger, J. Fink, S.-Z. Bruschetini-Ambro, Ermittlung der dynamischen Kennwerte von Eisenbahnbrücken unter Anwendung von unterschiedlichen Schwingungsanregungsmethoden. *Bauingenieur*, **92**, 2-13, 2017.

[15] C. Petersen, H. Werkle, *Dynamik der Baukonstruktionen, Vol. 2*. Springer Vieweg, Wiesbaden, 2017.

[16] A. Stollwitzer, J. Fink, T. Malik, Experimental analysis of damping mechanisms in ballasted track on single-track railway bridges. *Engineering Structures*, **220**, 110982, 2020.

[17] R. Behnke, M. Kaliske, Square block foundation resting on an unbounded soil layer: Long-term prediction of vertical displacement using a time homogenization technique for dynamic loading. *Soil Dynamics and Earthquake Engineering*, **115**, 448–471, 2018.

[18] C. Birk, R. Behnke, A modified scaled boundary finite element method for three-dimensional dynamic soil-structure interaction in layered soil. *International Journal for Numerical Methods in Engineering*, **89**, 371–402, 2012.

[19] E. Erduran, S. Gonen, B. Pulatsu, S. Soyoz, Damping in masonry arch railway bridges under service loads: An experimental and numerical investigation. *Engineering Structures*, **294**, 116801, 2023.

[20] V. Gattulli, E. Lofrano, A. Paolone, F. Potenza, Measured properties of structural damping in railway bridges. *Journal of Civil Structural Health Monitoring*, **9**, 639–653, 2019.

[21] A. Stollwitzer, J. Fink, Die rechnerische Bestimmung der Dämpfung von Stahl-Eisenbahnbrücken – Teil 1: Theorie. *Stahlbau*, **90**, 305–315, 2021.

[22] A. Stollwitzer, J. Fink, Die rechnerische Bestimmung der Dämpfung von Stahl-Eisenbahnbrücken – Teil 2: Verifizierung anhand von Bestandsbrücken. *Stahlbau*, **90**, 449–462, 2021.

[23] L. Bettinelli, *Comparison of Different Modeling Strategies for Dynamic Calculations of Railway Bridge Vibrations*. Doctoral Thesis, Faculty of Civil and Environmental Engineering, TU Wien, 2024.

[24] P.A. Montenegro, R. Silva, F. Pimenta, E. Laligant, C. Dos Santos, C. Laurent, Damping assessment on railway bridges based on an extensive experimental database framed on the InBridge4EU project. *Proceedings of the Sixth International Conference on Railway Technology: Research, Development and Maintenance*, Prague, September 1-5, 2024, DOI: 10.4203/ccc.7.15.3.